



# One-pot synthesis of graphene–chitosan nanocomposite modified carbon paste electrode for selective determination of dopamine



Chang Liu, Jing Zhang, Yifeng E., Jingli Yue, Lianshan Chen, Donghui Li \*

College of Pharmacy, Liaoning Medical University, Jinzhou 121001, PR China

## ARTICLE INFO

### Article history:

Received 14 January 2014

Accepted 28 April 2014

Available online 12 June 2014

### Keywords:

Dopamine

Selective determination

Surface modification of carbon paste electrode

Technique of one-pot synthesis

## ABSTRACT

**Background:** A simple, rapid, low-cost and environmentally friendly method was developed to determine dopamine (DA) in the presence of ascorbic (AA) and uric acid (UA) based on a novel technique to prepare a graphene–chitosan (GR–CS) nanocomposite and modify it on the surface of carbon paste electrode (CPE). For our design, CS acts as a media to disperse and stabilize GR, and then GR plays a key role to selective and sensitive determination of DA.

**Results:** Under physiological conditions, the linear range for dopamine was determined from  $1 \times 10^{-4}$  to  $2 \times 10^{-7}$  mol/L with a good correlation coefficient of 0.9961 in the presence of 1000-fold interference of AA and UA. The detection limit was estimated to be  $9.82 \times 10^{-8}$  mol/L ( $S/N = 3$ ). In order to study the stability and reproducibility, GR/CS/CPE underwent successive measurements in 10 times and then tested once a day for 30 d. The result exhibited 98.25% and 91.62% activities compared with the original peak current after 10-time measurements and 30-d storage.

**Conclusion:** The GR/CS/CPE has wide linear concentration range, low detection limit, and good reproducibility and stability, which suggests that our investigations provide a promising alternative for clinic DA determination.

© 2014 Pontificia Universidad Católica de Valparaíso. Production and hosting by Elsevier B.V. All rights reserved.

## 1. Introduction

Since we have known that dopamine (DA) plays a key role in the functions of human being, determinations of DA as an important basis of clinical diagnosis have attracted much interest [1,2]. Various methods have been developed to analysis of DA including chromatography, flow-injection chemiluminescence and electrolysis [3,4,5,6,7,8]. Among the methods mentioned above, electrochemical method presents distinctive advantages, such as quick response, low detection limit, low cost, simple operation and the absence of pretreatment. However, interferences of electroactive impurities, especially the interferences of ascorbic acid (AA) and uric acid (UA) that coexist with DA in body fluids, always affect the accuracy of determinations. In order to eliminate these interferences, the technique of chemically modified electrode has been used to determine DA selectively [9,10,11,12,13,14]. As mentioned from Pardavé's work, only

simple modification of the electrode surface with sodium dodecyl sulfate micelles has successfully provided a drastic change in the DA oxidation potential peak, and then the electrochemical oxidation overlap of DA, UA and AA has been separated [15].

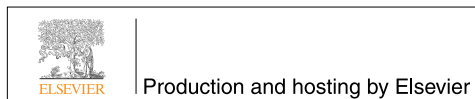
Attachment of nanomaterials to the surface of electrode has received wide attention because the modified electrode exhibits more favorable properties than bold electrode even simple chemical modification [16,17,18,19,20]. Graphene (GR), as a prototype two-dimensional carbon system, has been considered as an ideal nanomaterial for modified electrode. Particularly, GR that can provide a friend microenvironment is a promising alternative to bioassay [21,22,23,24,25,26,27,28]. Therefore attractive nature of GR permanently leads to extensive concerns for its synthesis and applications. Currently, several methods have been suggested to prepare GR, such as mechanical cleavage of graphite [29], chemical reduction of graphite oxide [30], thermal expanded graphite [31] and liquid-phase exfoliation [32]. Especially the last method, the liquid-phase exfoliation, is very appealing because it is direct, simple and has subsequent easy applications. Due to the strong  $\pi$ – $\pi$  stacking and Van der Waals interactions, the solvent choice referring to GR disperse and agglomerate became the key parameter for the technique of liquid-phase exfoliation [25].

The driving force in the investigations and applications of chitosan (CS) is from its satisfying film-forming ability, biodegradability and biocompatibility, especially as a naturally abundant product from deacetylation of chitin [33,34,35]. To the end, CS has been already

\* Corresponding author.

E-mail address: lidonghuix@sina.com (D. Li).

Peer review under responsibility of Pontificia Universidad Católica de Valparaíso.



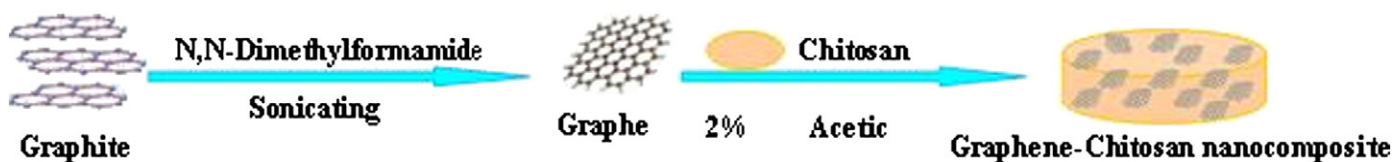


Fig. 1. The procedure for the synthesis of GR-CS nanocomposite.

used to disperse nanomaterials and coat biomacromolecules [36,37]. Undoubtedly, these intriguing investigations and relative background on the nanomaterials preparation encourage us to continue our efforts for the technique of liquid-phase exfoliation in a convenient and green way. Herein we successfully introduce CS to liquid-phase exfoliation of graphite towards stabilization and solubilization of GR in an aqueous dispersed system. Additionally, the excellent adsorption and viscosity of CS tightens GR modification on the surface of the object.

For this study, hybrid nanocomposite of GR-CS was synthesized by a simple step and then modified on the surface of carbon paste electrode (CPE). The results showed that this modified electrode owns the ability to selectively determine DA with high concentrations of interference. Moreover, this strategy for DA determination was quite accurate and stable. Therefore, the GR-CS modified CPE (GR/CS/CPE) could be a sort of inexpensive and rapid biosensor for DA determination and a good alternative to clinical diagnosis.

## 2. Experimental

### 2.1. Reagents and instruments

Dopamine hydrochloride was purchased from Sigma-Aldrich (Germany), and (+)-sodium L-ascorbate, uric acid and chitosan were obtained from Sigma-Aldrich (China). Graphite was obtained from Tianjin Chemical Reagent Factory (China). N,N-dimethylformamide was purchased from Sinopharm Chemical Reagent Co., Ltd (China). All the reagents used in this study were of analytical grade, and all solutions were prepared with distilled water. All electrochemical measurements were performed by a CHI650D workstation (Chenhua, Shanghai). A GR/CS/CPE fabricated for a working electrode, a platinum wire and an

Ag/AgCl electrode were used to complete the three-electrode system. All the experimental data were the average of three measurements.

### 2.2. Synthesis of GR-CS nanocomposite

The synthesis of GR-CS nanocomposite is described below: 30 mg graphite was continuously sonicated in 15 mL N,N-dimethylformamide for 30 min, and then 15 mL of 2% acetic acid solution was added for 10 min sonication. The GR-CS mixture was prepared by ultrasonic stirring 60 mg chitosan with the dispersion mentioned above for 1 h. Eventually the resultant dispersion was centrifuged for 90 min at 500 rpm.

### 2.3. Preparation of GR/CS/GPE

The CPE was prepared by mixing 440 mg graphite powder with 150 mg solid paraffin in an agate mortar and put in incubator until paraffin melted completely. Then the paste was packed into the end of a glass tube, and a copper wire was used as an electrical contact. The surface of the electrodes was polished with Sulfuric acid paper. Eventually, 20  $\mu$ L nanocomposite of GR-CS was cast to the polished surface of CPE and dried at room temperature.

## 3. Results and discussion

### 3.1. Preparation and characterization of GR-CS nanocomposite

GR-CS nanocomposite can be developed in one-pot based on Fig. 1 as described in Section 2.2. While using liquid-phase exfoliation, GR nanosheets show their perfect two-dimensional structure as transparent

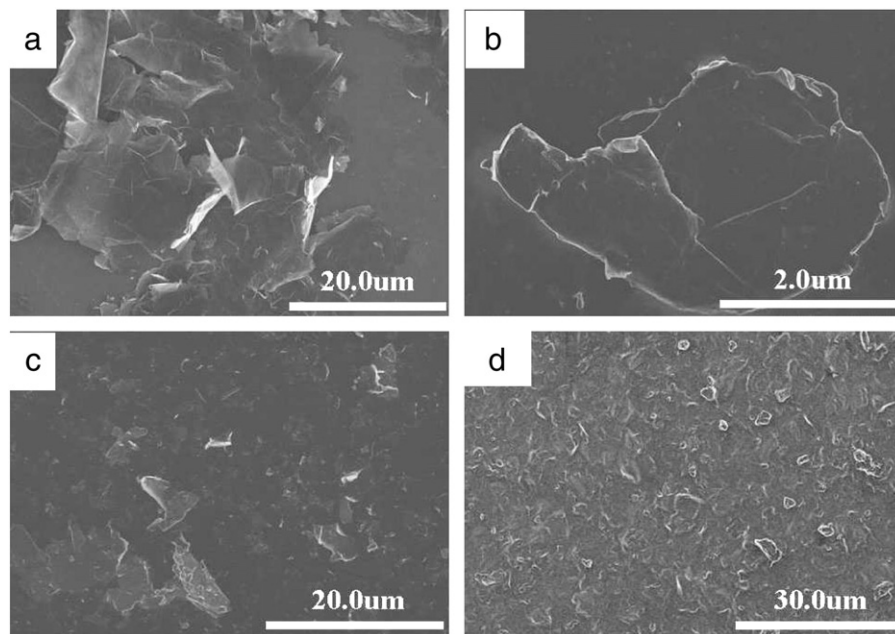
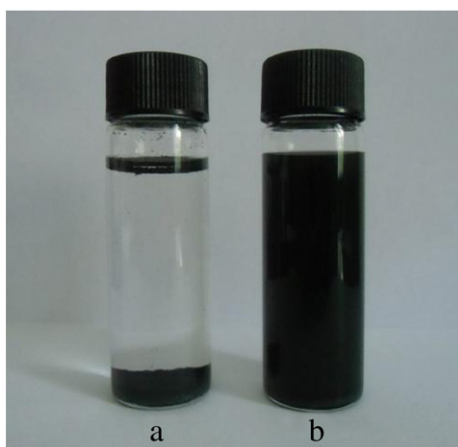
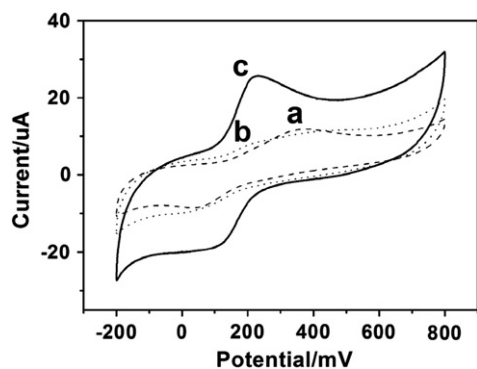


Fig. 2. The images of scanning electron microscope for GR synthesized by liquid-phase exfoliation in N,N-Dimethylformamide (a), one-pot synthesis of GR-CS nanocomposite at low magnification (b) and high magnification (c), GR-CS nanocomposite modified on the surface of CPE (d).



**Fig. 3.** Photographs of GR dispersed in N,N-dimethylformamide after 3 d store in room temperature (a), GR-CS nanocomposite solution after 21 d store at room temperature (b).



**Fig. 4.** CVs of bare carbon paste electrode (a: —), CS/CPE (b: .....), GR/CS/CPE (c: —) in 0.10 M phosphate buffer (pH 7) containing  $1 \times 10^{-4}$  mol/L DA. Scan rate:  $100 \text{ mV s}^{-1}$ .

paper (Fig. 2a). Unfortunately, the GR starts to re-agglomerate and settle down just for 3 d (Fig. 3a). Then CS was introduced into the process of exfoliation, and the GR-CS composite still exhibits its classical two-dimensional structure and disperses homogeneously (Fig. 2b). Moreover, the CS solution effectively avoids agglomeration and settlement of GR even during storage in 21 d (Fig. 3b). These results could be attributed to the special structure of CS. The intramolecular structure of CS that has both hydrophilic group and hydrophobic group facilitates itself and can be dissolved in dilute acid solution. Then the protonated amines make CS positively charged groups increasing in

diluted acid solution. Owing to a large amount of p electrons in  $sp^2$  hybrid orbital of carbon atom in GR, GR can be dispersed in CS solution homogeneously and stably. However, all sizes of GR-CS composite are obviously smaller than Fig. 2a (Fig. 2c). Fig. 2d proves the membrane of GR-CS nanocomposite coated on the surface of CPE evenly and tightly.

### 3.2. Electrochemical response of DA at the GR/CS/GPE

In order to study the advantages of the GR/CS/GPE for DA determination, the cyclic voltammograms (CVs) were used to compare the performance of the bare carbon paste electrode, CS/CPE and GR/CS/CPE, respectively. As shown in Fig. 4, the redox peak current of DA on the surface of CS/CPE is smaller than bare carbon paste electrode, but the redox peak current of DA significantly increases when the electrode surface is wrapped with GR-CS nanocomposite. Additionally, the  $\Delta E_p$  of the GR/CS/CPE is 119.23 mV which is smaller than other tested electrodes in our investigations. All results indicate that GR is the dominant factor of accelerating electron transfer on the electrode surface. However, CS plays a mass transfer barrier layer that inhibits the diffusion of the dopamine towards the electrode surface. According to another investigation, CS layer has been proven that it has its own ability to inhibit and even eliminate the response of the concomitants for dopamine determination [38].

### 3.3. Effects of pH

Differential pulse voltammograms (DPVs) were employed to detect the electrochemical behaviors of DA at the surface of GR/CS/CPE in 0.10 M phosphate buffer with different pH values (Fig. 5a). According to the results of DPVs, the largest current is obtained at pH 7 which closes to the physiological pH conditions. Therefore, pH 7 was chosen for the subsequent experiments and provided the possibility of real samples' determination. Fig. 5b shows the relationship of peak potential and pH. It can be seen that the peak potential of DA decreases obviously with the increase of pH, and the linear regression equation is  $E_{pa}(\text{mV}) = 552.38 - 49.45 \text{ pH}$  ( $R = -0.9911$ ). A slope of  $-49.45 \text{ mV/pH}$  indicates that the proportion of the electron and proton involved in the reactions is equal according to Nernst equation.

### 3.4. Effects of scan rate

Fig. 6a shows the CVs of  $1 \times 10^{-4}$  mol/L DA at the surface of GR/CS/CPE with different scan rates in the range of 20–200  $\text{mV s}^{-1}$ . Fig. 6b shows a good linear relationship between the anodic peak current and the square root of the scan rate. The linear regression equation is  $I(\text{uA}) = -7.32 + 3.45v^{1/2}$  ( $\text{mV s}^{-1})^{1/2}$ , and the correlation coefficient is 0.9979. According to the relationship gotten above, we can deduce that the reaction of electron transfer on the surface of GR/CS/CPE is controlled by a diffusive process.

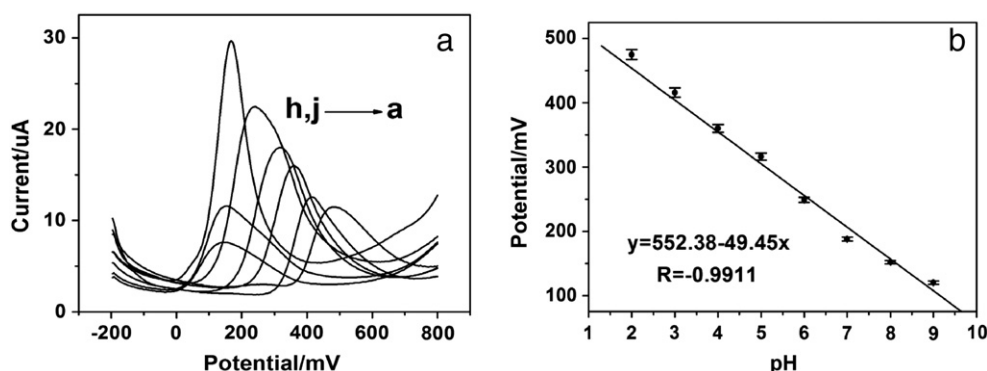


**Fig. 5.** DPVs of GR/CS/CPE in 0.1 M phosphate buffer containing  $1 \times 10^{-4}$  mol/L DA at different pH (a–h): 2.00, 3.00, 4.00, 5.00, 6.00, 7.00, 8.00, 9.00 (a); plot of  $E_{pa}$  versus pH changes (b).

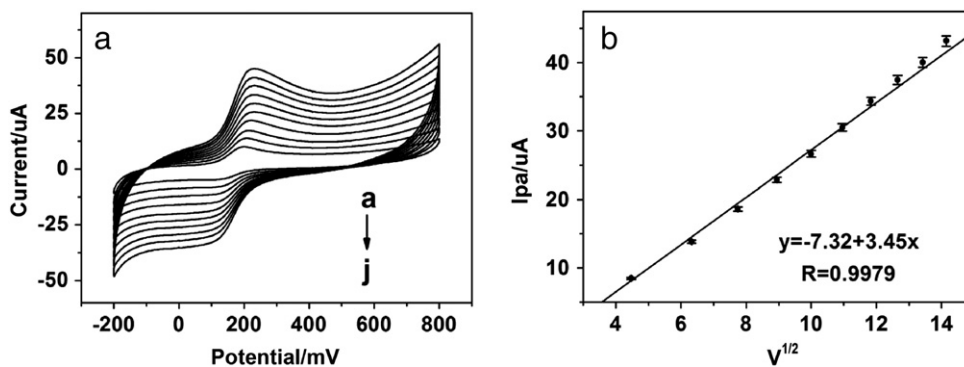


Fig. 6. CVs of GR/CS/CPE in 0.10 M phosphate buffer containing  $1 \times 10^{-4}$  mol/L DA at different scan rate: 20, 40, 60, 80, 100, 120, 140, 160, 180 and 200  $\text{mV s}^{-1}$  (a); Graph of anodic peak current versus the square root of the scan rate (b).

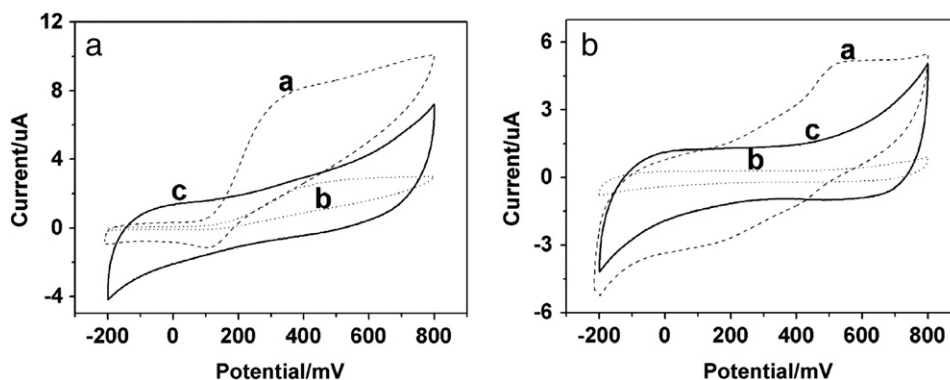


Fig. 7. CVs of bare carbon paste electrode (a: —), CS/CPE (b: .....), GR/CS/CPE (c: —) in 0.10 M phosphate buffer (pH 7) containing 0.10 mol/L AA (a); 0.10 mol/L UA (b). Scan rate: 100  $\text{mV s}^{-1}$ .

### 3.5. Electrochemical response of AA and UA at the GR/CS/GPE

In body fluids, AA and UA show 100–1000 times of concentrations compared with that of DA. So the selectivity of electrochemical determinations for DA is very important for clinic diagnosis. Fig. 7 shows the respective CVs of 0.10 mol/L AA and UA at bare CPE, CS/CPE and GR/CS/CPE. As shown in Fig. 7a and b, AA and UA obviously show oxidation peaks at 361 mV and 538 mV on the bare CPE, respectively. Then the chitosan was modified on the CPE, and the oxidation peak current of AA declines sharply and just appears as a relatively wide oxidation peak at 463 mV (Fig. 7a). The oxidation peak of UA even disappears (Fig. 7b). Following the modification of GR, the oxidation peak of AA can not be observed completely (Fig. 7a). The chemical

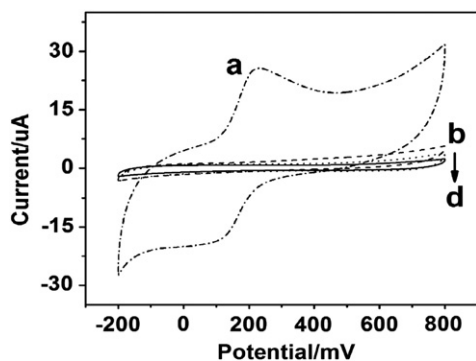


Fig. 8. CVs of scanned by GR/CS/CPE in the presence of  $1 \times 10^{-4}$  mol/L DA, 0.1 mol/L AA and UA. (a: -.-), 0.10 mol/L AA (b: ---), 0.10 mol/L UA (c: -) in 1.00 mol/L phosphate buffer (d: ...) at scan rate of 100  $\text{mV s}^{-1}$ .

modification is an effective way to eliminate inherent interference of AA and UA. A plausible explanation for this behavior can be in the references [15,39]. According with a lot of investigations, Pardavé considers that the changing of chemical behavior is relative to standard rate constants,  $k^0$ , for UA and AA, which must be drastically diminished on the modified surface of electrode.

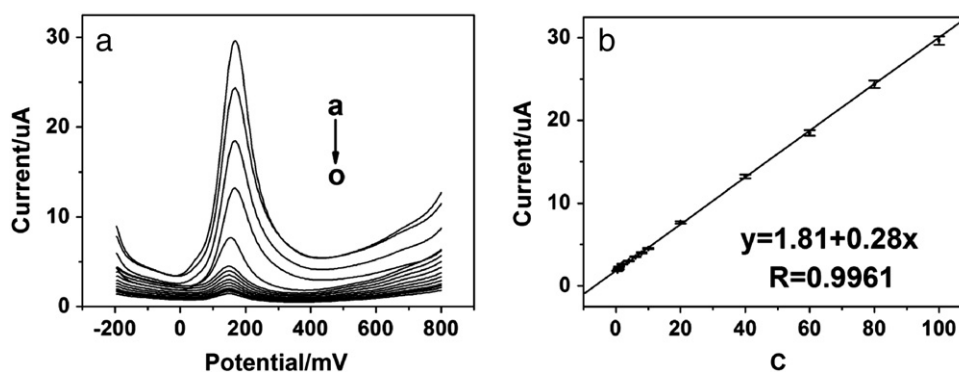
Fig. 8 shows the CVs of  $1 \times 10^{-4}$  mol/L DA with impurities of 0.10 mol/L AA and UA (a), 0.10 mol/L AA (b), 0.10 mol/L UA (c) and blank phosphate buffer (d) at the modified electrode with a scan rate of 100  $\text{mV s}^{-1}$ . In 1000 times presence of AA and UA compared with the DA, DA shows remarkable response with negligible background at the surface of GR/CS/CPE. The oxidation peak current ( $I_{pa}$ ) and  $E_{pa}$  of DA are 25.83  $\mu\text{A}$  and 231.91 mV which are extremely close to only the presence of DA ( $I_{pa}$  is 25.66  $\mu\text{A}$  and  $E_{pa}$  is 231.05 mV).

Fig. 9a shows the DPVs of different concentrations of DA in the presence of AA and UA. The DPV peak currents increase linearly with the increase of DA concentration over the range of 0.20–100  $\mu\text{mol/L}$ . The linear regression equation is  $I(\mu\text{A}) = 1.81 + 0.28C(\mu\text{mol/L})$ , and the correlation coefficient is 0.9961. Then the detection limit is  $9.82 \times 10^{-8}$  mol/L with noise–signal ratio in 3.

### 3.6. Stability and reproducibility

The stability and reproducibility of the GR/CPE and the GR/CS/GPE were investigated in the PBS solution containing  $1 \times 10^{-4}$  mol/L DA, and 0.10 mol/L AA and UA. According to successive measurements in 10 times, the relative standard deviation of the oxidation peak currents gotten by the GR/CPE and the GR/CS/GPE are 2.36% and 1.75%, respectively. The electrodes are stored in 4°C and tested once a d for 30 consecutive d, and the anodic peak currents of the GR/CPE





**Fig. 9.** DPVs of GR/CS/CPE in 0.1 M phosphate buffer containing different concentrations of 0.20, 0.40, 0.60, 0.80, 1, 2, 4, 6, 8, 10, 20, 40, 60, 80, 100  $\mu\text{mol/L}$  DA (a–o) in the presence of 1000-fold concentration of AA and UA (a); Calibrating plots of the anodic peak current versus DA concentrations (b).

exhibited only 72.32% activities compared with initial value, but those of the GR/CS/GPE exhibited more than 91.62% activities (Fig. 10). These mean that CS introduced to our modified electrode indeed improves the performance of stability.

#### 4. Concluding remarks

In this work, we overcome the traditional difficulties of GR preparation and storage, and a novel method of one-step to prepare GR–CS nanocomposites was developed. The GR–CS nanocomposite in our investigations shows a good two-dimensional carbon system and stability for 21 d storage. Then the GR–CS nanocomposite modified CPE exhibits an excellent performance for DA determination in the 1000 times interference of AA and UA at physiological pH. The brilliant characters of GR/CS/CPE, such as wide linear concentration range, low detection limit, and good reproducibility and stability, suggest that our investigations provide a promising alternative for clinic DA determination.

#### Conflict of interest

There are no conflict of interest.

#### Financial support

Agency/institution: Department of Education of Liaoning Province (L2011152). Program Financial support: Assistance of Doctor Research (Y2012B006). Project number: L2011152 and Y2012B006.

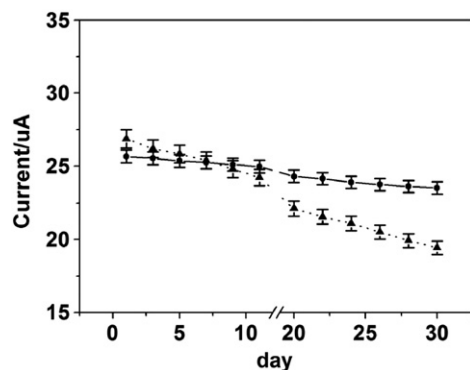


**Fig. 10.** Plot of the anodic peak current versus d (1–30 d) of GR/CPE (a:.....), GR/CS/CPE (b: -).

#### Acknowledgments

We acknowledge the financial support from the Department of Education of Liaoning Province (L2011152) and Assistance of Doctor Research (Y2012B006).

#### Author contributions

Proposed the theoretical frame: DL; Conceived and designed the experiments: CL; Software development: LC; Contributed reagents/materials/analysis tools: JY; Wrote the paper: CL; Performed the experiments: JZ; Analyzed the data: YE.

#### References

- [1] Heien MLAV, Khan AS, Ariansen JL, Cheer JF, Philips PEM, Wassum KM, et al. Real-time measurement of dopamine fluctuations after cocaine in the brain of behaving rats. *Proc Natl Acad Sci U S A* 2005;102:10023–8. <http://dx.doi.org/10.1073/pnas.0504657102>.
- [2] Wightman RM, May LJ, Michael AC. Detection of dopamine dynamics in the brain. *Anal Chem* 1988;60:769A–93A. <http://dx.doi.org/10.1021/ac00164a001>.
- [3] Karthikeyan K, Arularasu GT, Murali V, Pillai KC. Identification, isolation, characterization and response factor determination of process-related impurity in meprobamate drug substance. *J Pharm Biomed Anal* 2011;54:208–12. <http://dx.doi.org/10.1016/j.jpba.2010.07.018>.
- [4] Imperato A, Chiara GD. Trans-striatal dialysis coupled to reverse phase high performance liquid chromatography with electrochemical detection: A new method for the study of the *in vivo* release of endogenous dopamine and metabolites. *J Neurosci* 1984;4:966–77.
- [5] Church WH, Justice JB, Byrd LD. Extracellular dopamine in rat striatum following uptake inhibition by cocaine, nomifensine and benzotropine. *Eur J Pharmacol* 1987;139:345–8. [http://dx.doi.org/10.1016/0014-2999\(87\)90592-9](http://dx.doi.org/10.1016/0014-2999(87)90592-9).
- [6] Nalewajko E, Ramirez RB, Kojlo AJ. Determination of dopamine by flow-injection analysis coupled with luminol-hexacyanoferrate(III) chemiluminescence detection. *J Pharm Biomed Anal* 2004;36:219–23. <http://dx.doi.org/10.1016/j.jpba.2004.05.009>.
- [7] Zhou YP, Yan HL, Yan QJ, Huang SY, Liu JL, Li Z, et al. Simultaneous analysis of dopamine and homovanillic acid by high-performance liquid chromatography with wall-jet/thin-layer electrochemical detection. *Analyst* 2013;138:7246–53. <http://dx.doi.org/10.1039/c3an01437a>.
- [8] Peterson ZD, Collins DC, Bowerbank CR, Lee ML, Graves SW. Determination of catecholamines and metanephrines in urine by capillary electrophoresis–electrospray ionization–time-of-flight mass spectrometry. *J Chromatogr B* 2002;776:221–9. [http://dx.doi.org/10.1016/S1570-0232\(02\)00368-9](http://dx.doi.org/10.1016/S1570-0232(02)00368-9).
- [9] Chandra U, Swamy BEK, Gilbert O, Shergara BS. Voltammetric resolution of dopamine in the presence of ascorbic acid and uric acid at poly (calmagite) film coated carbon paste electrode. *Electrochim Acta* 2010;55:7166–74. <http://dx.doi.org/10.1016/j.electacta.2010.06.091>.
- [10] Jo S, Jeong H, Bae SR, Jeon S. Modified platinum electrode with phytic acid and single-walled carbon nanotube: Application to the selective determination of dopamine in the presence of ascorbic and uric acids. *Microchem J* 2008;88:1–6. <http://dx.doi.org/10.1016/j.microc.2007.08.005>.
- [11] Temocin Z. Modification of glassy carbon electrode in basic medium by electrochemical treatment for simultaneous determination of dopamine, ascorbic acid and uric acid. *Sens Actuators B* 2013;176:796–802. <http://dx.doi.org/10.1016/j.snb.2012.09.078>.
- [12] Liu Y, Huang JS, Hou HQ, You T. Simultaneous determination of dopamine, ascorbic acid and uric acid with electrospun carbon nanofibers modified electrode. *Electrochem Commun* 2008;10:1431–4. <http://dx.doi.org/10.1016/j.elecom.2008.07.020>.

- [13] Wang YZ, Zhong H, Li XM, Jia FF, Shi YX, Zhang WZ, et al. Perovskite LaTiO<sub>3</sub>-Ag<sub>0.2</sub> nanomaterials for nonenzymatic glucose sensor with high performance. *Biosens Bioelectron* 2013;48:56–60. <http://dx.doi.org/10.1016/j.bios.2013.03.081>.
- [14] Zhang L, Jiang X. Attachment of gold nanoparticles to glassy carbon electrode and its application for the voltammetric resolution of ascorbic acid and dopamine. *J Electroanal Chem* 2005;583:292–9. <http://dx.doi.org/10.1016/j.jelechem.2005.06.014>.
- [15] Colín-Orozco E, Ramírez-Silva MT, Corona-Avendano S, Romero-Romo M, Palomar-Pardavé M. Electrochemical quantification of dopamine in the presence of ascorbic acid and uric acid using a simple carbon paste electrode modified with SDS micelles at pH 7. *Electrochim Acta* 2012;85:307–13. <http://dx.doi.org/10.1016/j.electacta.2012.08.081>.
- [16] Mao Y, Bao Y, Gan SY, Li FH, Niu L. Electrochemical sensor for dopamine based on a novel graphene-molecular imprinted polymers composite recognition element. *Biosens Bioelectron* 2011;28:291–7. <http://dx.doi.org/10.1016/j.bios.2011.07.034>.
- [17] Guo YJ, Li J, Dong SJ. Hemin functionalized graphene nanosheets-based dual biosensor platforms for hydrogen peroxide and glucose. *Sens Actuators B* 2011;160:295–300. <http://dx.doi.org/10.1016/j.snb.2011.07.050>.
- [18] Sun B, Zhang K, Chen LJ, Guo LT, Ai SY. A novel photoelectrochemical sensor based on PPIX-functionalized WO<sub>3</sub>-rGO nanohybrid-decorated ITO electrode for detecting cysteine. *Biosens Bioelectron* 2013;44:48–51. <http://dx.doi.org/10.1016/j.bios.2013.01.014>.
- [19] Gan WY, Zhao HJ. Photoelectrocatalytic activity of mesoporous TiO<sub>2</sub> thin film electrodes. *Appl Catal A* 2009;354:8–16. <http://dx.doi.org/10.1016/j.apcata.2008.10.054>.
- [20] Qiu JX, Zhang S, Zhao HJ. Recent applications of TiO<sub>2</sub> nanomaterials in chemical sensing in aqueous media. *Sens Actuators B* 2011;160:875–90. <http://dx.doi.org/10.1016/j.snb.2011.08.077>.
- [21] Geim AK, Novoselov KS. The rise of graphene. *Nat Mater* 2007;6:183–91. <http://dx.doi.org/10.1038/nmat1849>.
- [22] Fowler JD, Allen MJ, Tung VC, Yang Y, Kaner RB, Weiller BH. Practical chemical sensors from chemically derived graphene. *ACS Nano* 2009;3:301–6. <http://dx.doi.org/10.1021/nn800593m>.
- [23] Qiu JX, Zhang P, Ling M, Li S, Liu P, Zhao H, et al. Photocatalytic synthesis of TiO<sub>2</sub> and reduced graphene oxide nanocomposite for lithium ion battery. *ACS Appl Mater Interfaces* 2012;4:3636–42. <http://dx.doi.org/10.1021/am300722d>.
- [24] Li D, Kaner RB. Graphene-based materials. *Science* 2008;320:1170–1. <http://dx.doi.org/10.1126/science.1158180>.
- [25] Li D, Muller MB, Gilje S, Kaner RB, Wallace GG. Processable aqueous dispersions of graphene nanosheets. *Nat Nanotechnol* 2008;3:101–5. <http://dx.doi.org/10.1038/nnano.2007.451>.
- [26] Westervelt RM. Graphene nanoelectronics. *Science* 2008;320:324–5. <http://dx.doi.org/10.1126/science.1156936>.
- [27] Guo YJ, Deng L, Li J, Guo SJ, Wang EK, Dong SJ. Hemin-graphene hybrid nanosheets with intrinsic peroxidase-like activity for label-free colorimetric detection of single-nucleotide polymorphism. *ACS Nano* 2011;5:1282–90. <http://dx.doi.org/10.1021/nn1029586>.
- [28] Guo YJ, Guo SJ, Ren JT, Zhai YM, Dong SJ, Wang EK. Cyclodextrin functionalized graphene nanosheets with high supramolecular recognition capability: Synthesis and host-guest inclusion for enhanced electrochemical performance. *ACS Nano* 2010;4:4001–10. <http://dx.doi.org/10.1021/nn100939n>.
- [29] Novoselov KS, Geim AK, Morozov SV, Jiang D, Zhang Y, Dubonos SV, et al. Electric field effect in atomically thin carbon films. *Science* 2004;306:666–9. <http://dx.doi.org/10.1126/science.1102896>.
- [30] Stankovich S, Dikin DA, Piner RD, Kohlhaas KA, Kleinhammes A, Jia YY, et al. Synthesis of graphene-based nanosheets via chemical reduction of exfoliated graphite oxide. *Carbon* 2007;45:1558–65. <http://dx.doi.org/10.1016/j.carbon.2007.02.034>.
- [31] Dideikin AT, Sokolov VV, Sakseev DA, Baidakova MV, Vul AY. Free graphene films obtained from thermally expanded graphite. *Technol Phys* 2010;55:1378–81. <http://dx.doi.org/10.1134/S1063784210090239>.
- [32] Hernandez Y, Nicolosi V, Lotya M, Blighe FM, Sun ZY, De S, et al. High-yield production of graphene by liquid-phase exfoliation of graphite. *Nat Nanotechnol* 2008;3:563–8. <http://dx.doi.org/10.1038/nnano.2008.215>.
- [33] Mageti NV, Kumar R. A review of chitin and chitosan applications. *React Funct Polym* 2000;46:1–27. [http://dx.doi.org/10.1016/S1381-5148\(00\)00038-9](http://dx.doi.org/10.1016/S1381-5148(00)00038-9).
- [34] Pheachamud T, Charoenteeraboon J. Antibacterial activity and drug release of chitosan sponge containing doxycycline hyclate. *AAPS PharmSciTech* 2008;9:829–35. <http://dx.doi.org/10.1208/s12249-008-9117-x>.
- [35] Chatelet C, Damour O, Domard A. Influence of the degree of acetylation on some biological properties of chitosan films. *Biomaterials* 2001;22:261–8. [http://dx.doi.org/10.1016/S0142-9612\(00\)00183-6](http://dx.doi.org/10.1016/S0142-9612(00)00183-6).
- [36] Yang SL, Luo SL, Liu CB, Wei WZ. Direct synthesis of graphene-chitosan composite and its application as an enzymeless methyl parathion sensor. *Colloids Surf B Biointerfaces* 2012;96:75–9. <http://dx.doi.org/10.1016/j.colsurfb.2012.03.007>.
- [37] Liu Y, Yang SL, Niu WF. Simple, rapid and green one-step strategy to synthesis of graphene/carbon nanotubes/chitosan hybrid as solid-phase extraction for square-wave voltammetric detection of methyl parathion. *Colloids Surf B Biointerfaces* 2013;108:266–70. <http://dx.doi.org/10.1016/j.colsurfb.2013.03.003>.
- [38] Wang Y, Li YM, Tang LH, Lu J, Li JH. Application of graphene-modified electrode for selective detection of dopamine. *Electrochim Commun* 2009;11:889–92. <http://dx.doi.org/10.1016/j.elecom.2009.02.013>.
- [39] Aldana-González A, Palomar-Pardavé M, Corona-Avendano S, Montes De Oca MG, Ramírez-Silva MT, Romero-Romo M. Gold nanoparticles modified-ITO electrode for the selective electrochemical quantification of dopamine in the presence of uric and ascorbic acids. *J Electroanal Chem* 2013;706:69–75. <http://dx.doi.org/10.1016/j.jelechem.2013.07.037>.